applied sciences

MDPI

Article

Supercapacitor-Based Energy Storage in Elevators to Improve Energy Efficiency of Buildings

Martin Makar, Luka Pravica * and Martina Kutija

Faculty of Electrical Engineering and Computing, University of Zagreb, Unska 3, 10000 Zagreb, Croatia; martin.makar@fer.hr (M.M.); martina.kutija@fer.hr (M.K.)
* Correspondence: luka.pravica@fer.hr

Abstract: Improving energy efficiency is the most important goal for buildings today. One of the ways to increase energy efficiency is to use the regenerative potential of elevators. Due to the special requirements of elevator drives, energy storage systems based on supercapacitors are the most suitable for storing regenerative energy. This paper proposes an energy storage system consisting of a supercapacitor bank and a bidirectional six-phase interleaved DC/DC converter. The energy savings achieved by the proposed system were investigated through simulation tests. The proposed system was modeled considering all physical constraints. A simulation model of the existing faculty elevator system was created in PLECS and verified with field measurements. Reliable results were ensured by using the verified simulation model and considering all physical constraints. The operation of the proposed energy storage system was tested under various conditions. In addition, the simulation model of the elevator system with the proposed energy storage system was tested using the elevator traffic data obtained from the measurements. The simulation results show the effectiveness of the proposed energy storage system and that significant energy savings can be achieved.

Keywords: energy storage; efficiency; elevator; supercapacitor; regenerative energy

Citation: Makar, M.; Pravica, L.; Kutija, M. Supercapacitor-Based Energy Storage in Elevators to Improve Energy Efficiency of Buildings. *Appl. Sci.* **2022**, *12*, 7184. https://doi.org/10.3390/app12147184

Academic Editor: Francesco Salamone

Received: 11 June 2022
Accepted: 15 July 2022
Published: 16 July 2022

1. Introduction

Energy consumption in commercial, residential, and administrative buildings accounts for a significant portion of total energy consumption [1]. In order to increase savings in buildings and meet future climate and energy goals, the concepts of zero energy buildings (ZEBs) and positive energy buildings (PEBs) have been introduced [2,3]. The basic principle of these concepts is to optimize the energy consumption of buildings by using sustainable technologies and to generate energy by integrating renewable energy generation systems, resulting in buildings that can meet their energy needs and even generate more energy than is required. By implementing these concepts, the problems of energy-saving, environmental protection and reduction in CO_2 emissions in buildings are addressed, and reliability, independence from the power grid, environmental friendliness and cost efficiency are achieved [4,5].

The main goal of energy-efficient buildings is to keep energy consumption as low as possible. However, little attention has been paid to energy-efficient elevator systems, which can lead to significant energy savings in buildings [6]. Elevators typically account for 2% to 10% of a building's energy consumption [7], but, in high-rise buildings, they can reportedly be responsible for 17% to 25% of total energy consumption [8]. During peak periods, elevators can consume up to 40% of a building's energy [9]. In addition, elevators can generate clean energy that can be used for consumers in the building instead of being wasted as heat, as is the case with conventional elevator systems. According to [10], there is significant potential for savings in elevator systems that can be realized through numerous measures: reducing standby consumption, adapting new motor technologies, using regenerative energy, improving dispatching systems, or introducing machine-roomless

(MRL) approaches. By implementing these measures, energy savings of 40% or more can be achieved [11]. Research on the development of a net-zero energy elevator concept has also been reported [7].

Recently, energy savings in elevator systems achieved through the use of regenerative energy have attracted much attention. The most attractive solutions are energy storage systems connected to the DC-link of an elevator drive, where regenerative energy is stored and can be used to reduce peak loads or supply other equipment. The solutions proposed in the literature are mainly based on supercapacitors. Supercapacitors have a high power density, a fast charge/discharge rate, a high number of charge/discharge cycles, and a long lifetime, making them suitable for elevator applications characterized by a high number of starts and stops, short trips, and high braking power in regenerative mode [12]. Typical designs of energy storage systems in elevator applications use a bidirectional DC/DC converter and a supercapacitor bank [8,13–23]. The research studies presented in the literature focus on control strategies [15,17], storage system design [13,14,18–22], supercapacitor bank sizing [8,19,21], DC/DC converter topology [23,24], and additional functions, such as emergency power supply [14] or power factor correction [16], with simulations and experimental tests used to validate the proposed concepts. However, a comprehensive estimation of the energy savings achieved by energy storage systems is missing.

In addition, only a few recent research papers have highlighted the role of energy-efficient elevators in improving building energy efficiency. In [25], a hybrid energy storage system with an ultracapacitor energy storage system and a battery energy storage system was proposed to reduce the power and energy consumption of elevators in residential buildings. An ultracapacitor was used to reduce peak consumption, and a battery storage system was used to supply the general electrical loads in the building. The proposed method was verified in MATLAB, focusing on an indirect field-oriented control strategy for the drive. However, the elevator traffic and characteristic parameters of the elevator speed profile were not considered. In [26], an energy-saving approach was proposed for a group of elevators based on a DC microgrid. An energy-efficient device based on supercapacitors was developed for the elevator group, and experimental tests showed that the energy savings ranged from 15.9 to 23.1% and 24.1 to 54.5% depending on the experiments conducted. However, details of the energy-efficient device and experiments were not provided. Therefore, the importance of energy-efficient elevators in improving a building's energy efficiency is gaining increasing attention. However, a comprehensive study of energy savings is still pending.

This paper proposes a supercapacitor-based energy storage system for elevator applications, consisting of a six-phase interleaved DC/DC converter and a supercapacitor bank. The objective of the paper is to evaluate the effectiveness of the proposed system and to estimate, as accurately as possible, the energy savings achieved. A comprehensive study of the energy savings obtained was performed using PLECS software. Since the proposed energy storage system was being prototyped, the simulation model of the energy storage system was built using its actual parameters and considering all physical constraints. In addition, the existing faculty elevator system was modeled, and the simulation model was verified using field measurements. Using the verified model of the existing elevator system, and considering all practical constraints in modeling the energy storage system, a complex simulation model was built to estimate the energy savings. The performance of the energy storage system and the achievable energy savings were analyzed under different operating conditions. Selected experimental results were evaluated to confirm the effectiveness of the proposed solution. The energy savings during a reference cycle, two consecutive regenerative trips, and considering actual elevator traffic data obtained from field measurements, were recorded and analyzed. Using the actual elevator traffic data, an estimate of the energy savings was found to be very close to the actual measurements. The energy consumption of the elevator system, with and without the energy storage system,

was compared. The results showed that the proposed energy storage system was able to achieve significant energy savings.

The paper is organized as follows: Section 2 describes the elevator system, and Section 3 describes the modeling and verification of the elevator system. The proposed energy storage system is presented in Section 4. The simulation results are presented in Section 5 and the discussion in Section 6. The conclusions are provided in Section 7.

2. Elevator System

The main components of a traction sheave elevator system are the car, the counterweight, the guides, and the electric drive [27]. The car and counterweight slide on guide rails and are connected by a suspension rope. The suspension rope is suspended from a traction sheave, driven by an electric drive. A typical elevator system is shown in Figure 1. A variable frequency drive (VFD) controls the electric drive [28]. Induction motors or permanent magnet motors are commonly used. The weight of the counterweight is usually selected to be equal to the sum of the weight of the empty car and 50% of the nominal load [27]. Thus, the elevator is in equilibrium when loaded with half the nominal load. The elevator system also includes mechanical safety devices for emergencies.

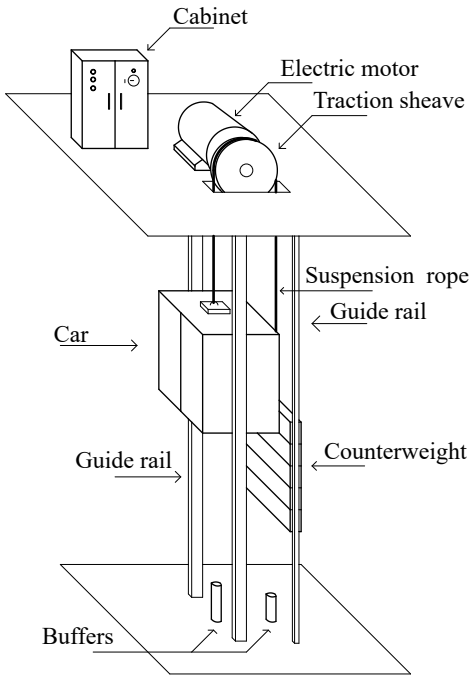

Figure 1. Elevator system.

The elevator drive can operate in motor mode and generator mode. In motor mode, the electric drive draws energy from the grid, while in generator mode it generates electrical energy that can be fed back into the grid or stored and used as needed. In conventional elevator systems, the regenerative energy is dissipated as heat at the braking resistor.

The operating mode of the elevator drive depends on the current difference in the total weight between the car and the counterweight and the direction of motion. The conditions for the operating modes are given in Table 1, where m_{tc} is the total weight of the car, including any passengers, and m_{cw} is the weight of the counterweight. When the total weight of the car and the weight of the counterweight are equal, the system is in equilibrium. However, the elevator drive operates in motor mode because it must compensate for mechanical losses (e.g., friction).

Table 1. Elevator drive operating modes.

Mode	Direction	Weight Ratio
Motor	Up	$m_{tc} > m_{cw}$
	Down	$m_{tc} < m_{cw}$
	Up or Down	$m_{tc} = m_{cw}$ *
Generator	Up	$m_{tc} < m_{cw}$
	Down	$m_{tc} > m_{cw}$

* Covering friction losses.

The energy consumption of an elevator is not easy to estimate, as it depends on several factors: the traffic demand, which is difficult to estimate, the dispatching system, the control system, the standby operation, etc. To estimate the annual consumption of an elevator and its energy efficiency, the most commonly used standards are VDI 4707 and ISO 25745 [29]. These standards are based on short-term energy measurements, where the energy consumption is measured during reference cycles. The reference cycle of an elevator consists of the trip from the ground floor to the top floor and back, starting and ending with an open door. The typical speed profile of an elevator during a reference cycle is shown in Figure 2.

Elevators usually travel at a constant speed and have an S-shaped speed when accelerating and decelerating to ensure passenger comfort. They enter the station at a very low speed, called the landing speed.

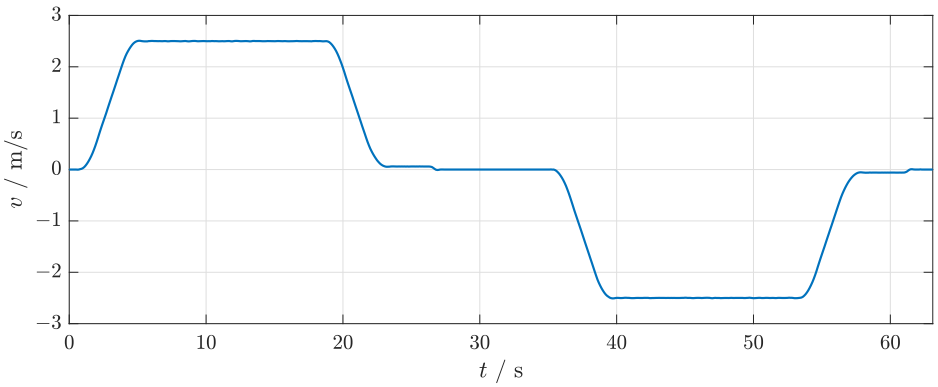

Figure 2. Example of elevator speed during the reference cycle.

3. Elevator System Modeling and Verification

To test the proposed energy storage system, the existing faculty elevator system was modeled in Plexim PLECS. The PLECS software is a simulation platform for power electronic systems that can model and simulate electrical, magnetic, thermal, and mechanical aspects of complete systems, including power sources, power converters, and loads. The PLECS library includes models of electrical machines (induction and synchronous machines), power electronic devices (semiconductors, such as IGBT and MOSFET), and thermal and mechanical components.

The proposed energy storage system consists of the VFD, the electrical machine, and the mechanical system. The simulation model of the elevator system is shown in Figure 3. The parameters of the elevator are given in Table A1, the parameters of the VFD are given in Table A2 and the parameters of the synchronous motor with permanent magnets are given in Table A3. The model of the three-phase synchronous machine with surface-mounted permanent magnets was used from the PLECS library, while the model of the elevator VFD and the elevator mechanical system were built manually. The models of the VFD and the mechanical system are described as follows.

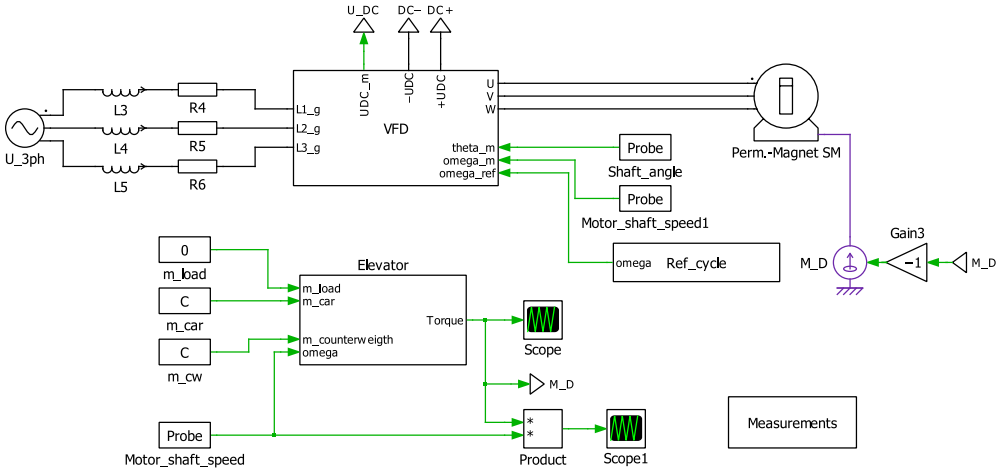

Figure 3. Elevator system simulation model in PLECS.

3.1. Mechanical System

The elevator mechanical system was modeled based on available faculty elevator data. The suspension ratio was 2:1, and the mass of the counterweight was 50% of the nominal load plus the mass of the empty car. The mass of the suspension rope, the mass of the traveling cable, and the mass of the compensation rope, as well as their dynamics, were assumed to be negligible.

The electric machine controls the mechanical system of the elevator. The torque of the electric machine was calculated as follows:

$$T_{\mathrm{m}} = F_{\mathrm{tot}} \cdot R + J_{\mathrm{tot}} \cdot \frac{d\omega}{dt} + D \cdot \omega \tag{1}$$

where T_m is the torque of the electric machine, F_{tot} is the total force on the traction sheave, R is the radius of the traction sheave, J_{tot} is the total moment of inertia, ω is the angular velocity of the machine shaft, and D is the damping factor of the mechanical system.

The total force F_{tot} depends on the weight difference between the car with any passengers on one side and the counterweight on the other. All mechanical system losses were accounted for with a damping factor D estimated from the efficiency of the mechanical system at nominal load. The input signals of the simulation model were the mass of the load (m_l) and the speed of the electric machine (ω), and the output signal was the torque of the electric machine (T_{m}).

3.2. VFD Model

The schematic of the VFD modeled in PLECS is shown in Figure 4. It consists of a three-phase diode rectifier, DC-link with capacitor C4 and inductors L1 and L2, and the inverter. Resistor R serves as a precharge resistor for capacitor C4. Since the three-phase diode rectifier cannot feed energy back to the grid during regenerative braking, this energy is dissipated at the braking resistor connected to terminals *B*+ and *B*–. Transistor T7 controls the heat dissipation at the braking resistor. The proposed EESS is connected to the +UDC and -UDC terminals, as shown in Figure 4.

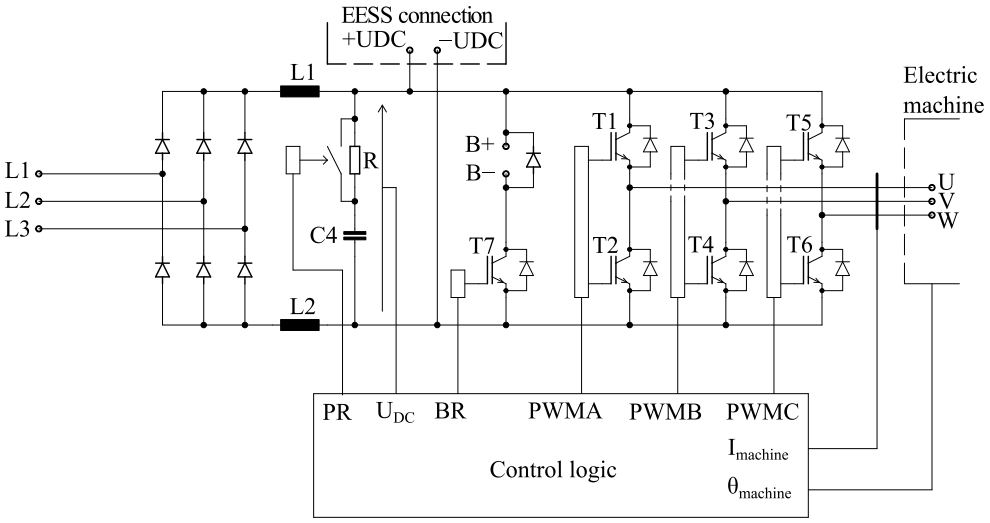

Figure 4. Schematic of the elevator VFD.

The VFD is supplied by a three-phase system with a line voltage of 400 V/50 Hz. The expected nominal voltage of the DC bus is therefore 565 V, but may vary between 500 V and 800 V (depending on the load and mains conditions), as this is the typical operating voltage of commercially available VFDs.

The control logic block is used to control the inverter, transistor T7, and the precharge circuit. The precharge resistor R is short-circuited with a delay of 1 s after the supply voltage is connected to the input of the VFD. Transistor T7 turns on when the voltage of the DC bus is higher than 720 V, and turns off when the voltage of the DC bus is lower than 700 V. The speed control of the electric machine is achieved with a field-oriented control (FOC) using a speed sensor. The schematic of the implemented FOC is shown in Figure 5.

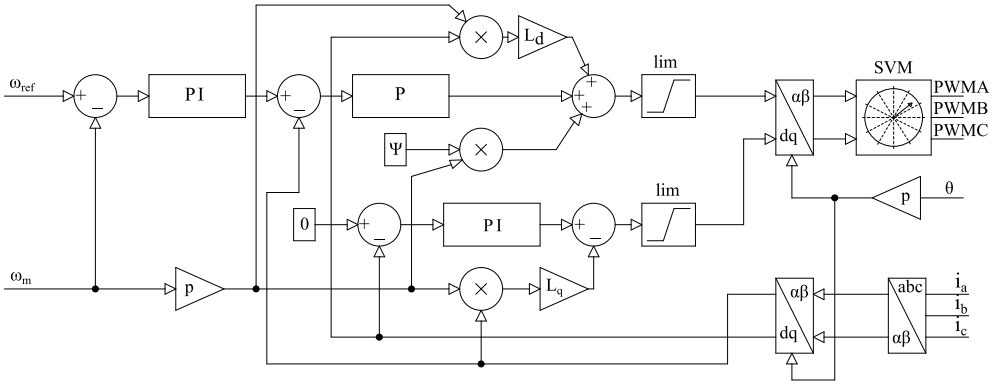

Figure 5. Schematic of the FOC.

The speed control of a synchronous machine with permanent magnets is based on the control structure proposed in [30]. A P controller is used in the current control loop and a PI controller in the speed control loop, while a PI controller is used to control the I_d current to eliminate the steady-state error [30]. Additional functions, such as anti-windup, current and voltage limiting, and field weakening were not modeled to reduce the complexity of the simulation model.

In a typical elevator application, a mechanical brake is installed. When the elevator car stops, the brake closes and prevents further movement of the motor shaft. Therefore, the electric motor is not used in standby mode. Before the elevator car is set in motion, a control system sets the torque setpoint of the electric motor based on the load measurement. When the brake is released, the electric motor smoothly overtakes the load, and the elevator car starts moving. A mechanical brake function was not implemented in the simulation

model. The motor constantly develops torque, even in standby mode, and the value of the torque is load-dependent.

3.3. Simulation Model Verification

The simulation model of the faculty elevator system shown in Figure 3 was verified by field measurements. The simulation model was fed with the speed and load profile of the faculty elevator obtained from the measurements, and the simulation results were compared with the measurements for different load and speed profiles. The comparison showed that the simulation model of the faculty elevator reproduced its actual behaviour very well and could be used for further analysis.

The results of the simulation test and the measurement test were compared for the elevator trip from the top floor to the ground floor and back with an empty car. The velocity profile during the test is shown in Figure 2. The power of the elevator system obtained by simulation and measurements is shown in Figure 6. In motor mode, the power corresponds to the power required by the grid; in generator mode, the power corresponds to the power fed back into the VFD. Since the VFD has a diode bridge rectifier, the power in generator mode was measured at DC-link, both in the measurement and simulation tests.

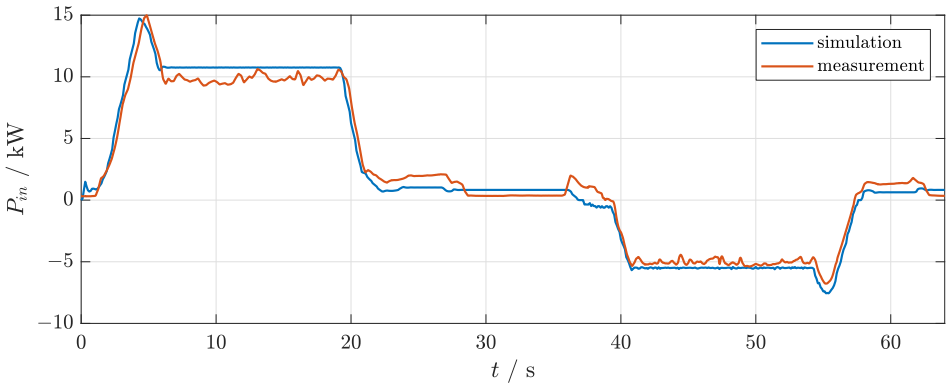

Figure 6. Comparison of power of the elevator system obtained from simulation and measurement.

4. Energy Storage System

The supercapacitor-based elevator energy storage system (EESS) proposed in this paper consists of a supercapacitor (SC) bank and a six-phase interleaved bidirectional DC/DC converter. The schematic of the EESS is shown in Figure 7. The EESS is connected to the DC bus of the VFD, and energy is transferred from the elevator to the SC bank and vice versa via a bidirectional DC/DC converter. An SC bank serves as energy storage.

The EESS was designed for an elevator drive with a nominal power of 10 kW. The 6-phase interleaved DC/DC converter was proposed to achieve the desired maximum output current ripple, reduce the volume of inductor and reduce the DC/DC converter losses. The SC bank was sized according to the regenerative energy potential analysis presented in [29,31]. The EESS simulation model consisted of the DC/DC converter, the SC bank, and the EESS control algorithm. The EESS simulation model was designed considering all physical constraints, which are explained in detail in the following subsections.

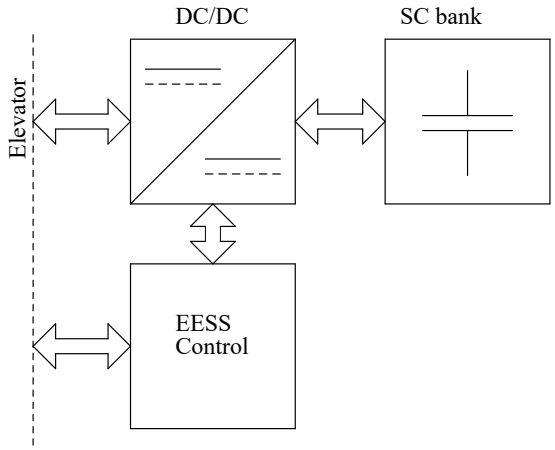

Figure 7. Schematic of supercapacitor-based EESS.

4.1. Supercapacitor Bank

The nominal voltage of the SC bank is typically in the range of 100 V to 300 V [14,18]. Considering that the nominal operating voltage of the VFD DC bus is 565 V and the non-isolated topology of the DC/DC converter is best suited for a transform ratio of 4 or less [32], the nominal voltage of the SC bank of 300 V was selected. The operating voltage range for the SC bank is usually selected in the range of $U_n/2$ to U_n, where U_n is the nominal voltage. In this way, 75 % of the total energy stored in the supercapacitors is used [14]. The selected operating voltage range for the SC bank is thus between 150 V and 300 V DC.

Since the typical nominal voltage of a supercapacitor cell is in the range of 1.2 V to 3.5 V [33], several supercapacitor cells must be connected in series to form an SC bank. The capacitance tolerance of each supercapacitor cell can vary between ±20% of nominal [34], which can result in uneven voltage distribution across the series-connected supercapacitor cells and higher than expected voltages across the supercapacitor cells. Higher than nominal voltages can lead to higher leakage currents, increased gassing, and overall destruction of the supercapacitor cells [35]. To solve the problem of uneven voltage distribution on supercapacitors, balancing circuits are used. Considering the complexity of the overall model and the complexity of the balancing circuits of supercapacitors, supercapacitor cells with the same characteristics are used to model the supercapacitor bank. Their series representation can be modeled as a supercapacitor with higher nominal voltage.

Supercapacitors are non-linear elements because their capacitance changes with voltage and frequency [34]. Several models of supercapacitors can be found in the literature [34,36,37]. The most accurate model of a supercapacitor is the transmission line model [36], which is very complex. In this paper, the supercapacitor bank was modeled as an ideal capacitor with ESR due to the high demands on the execution of the entire simulation model. The SC bank was sized to store energy for a maximum of two regenerative energy cycles. For the studied elevator, the maximum continuous regenerative power was 5.5 kW. The maximum regenerative energy was determined from field measurements and was 86 kJ, so the SC bank would be able to store at least 172 kJ.

The energy stored in the supercapacitor bank that can be further used can be calculated as follows:

$$E_{us} = \frac{U_n^2 \cdot C}{2} \cdot 0.75 \quad (2)$$

where U_n is the nominal voltage of the charged supercapacitor bank and C is the capacitance of the supercapacitor bank. The energy is multiplied by 0.75 since 75 % of the energy stored in the supercapacitor is used. Using the Equation (2) and the known maximum voltage of the supercapacitor bank, the required minimum capacitance of the supercapacitor bank was calculated to be 5.1 F.

Commercially available supercapacitor cells that could be used to form the supercapacitor bank have a nominal voltage of 2.7 V to 3 V. In [38], it is reported that charging a supercapacitor cell with 200 mV above the nominal voltage can shorten the lifetime of the supercapacitor by 64 times. It was also shown that it is possible to extend the lifetime of the supercapacitor cell if the operating voltage of the supercapacitor cell is kept below the nominal voltage. Thus, with a nominal voltage of 300 V selected for the supercapacitor bank in this paper, 120 supercapacitor cells with a nominal voltage of 2.7 V are required, and each cell should be charged to a maximum of 2.5 V. The minimum required capacitance of a cell can be calculated as follows:

$$C_{\text{cell\_min}} = N \cdot C_{\text{SC\_bank}} \tag{3}$$

where N is the number of supercapacitor cells connected in series and $C_{\text{SC\_bank}}$ is the minimum required capacitance of the supercapacitor bank. For the elevator under study, the minimum required capacitance of each cell must be 612 F. In this capacitance range, commercially available cells have a nominal capacitance value of 400 F, 600 F, or 1100 F. Therefore, it is assumed that the supercapacitor bank should consist of 400 F cells connected in parallel to achieve an equivalent capacitance of 800 F. When 120 supercapacitors of 800 F are connected in series, the nominal capacitance of the supercapacitor bank is 6.7 F, which is 31 % more than the calculated minimum capacitance of the supercapacitor bank.

For supercapacitor bank modeling, it is assumed that the supercapacitor bank consists of 240 cells of 400 F/2.7 V in parallel and series connection. The ESR of 400 F supercapacitor cells is about 3 mΩ, and it is assumed that, when two supercapacitor cells are connected in parallel, their ESR is 1.5 mΩ. When 120 supercapacitor pairs are connected in series, the equivalent ESR is 180 mΩ. The equivalent model used to model the SC bank is shown in Figure 8. All the supercapacitor bank parameters used for modeling are given in Table 2.

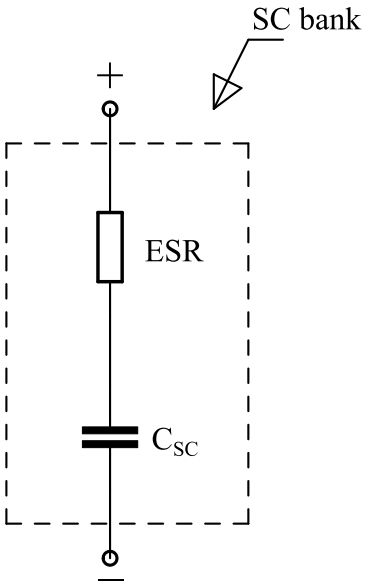

Figure 8. Equivalent model of the SC bank.

Table 2. SC bank parameters.

Parameter	Value
Operating voltage range, U_{ovr} [V]	150–300
Usable stored energy, E_{us} [kJ]	226
Total capacitance, C_{tot} [F]	6.7
ESR [mΩ]	180

In elevator applications, there are cases where the SC bank needs to be charged/discharged quickly at higher currents (e.g., 20 A in this case). Higher currents increase the losses caused by the ESR of the supercapacitor. The ESR value depends on the frequency and temperature [34]. As stated in [34], the ESR can be represented by a fixed value for modeling losses in elevator applications. Each supercapacitor manufacturer usually specifies a constant RMS current value where the supercapacitor temperature rise is within tolerance and does not significantly affect the supercapacitor characteristics. For a 400 F supercapacitor cell, the recommended maximum RMS current value is about 20–30 A, depending on the manufacturer and the desired temperature rise. Assuming that two cells are connected in parallel, and the current is evenly distributed, the maximum continuous current capacity of the SC bank is about 40–50 A.

4.2. DC/DC Converter

For bidirectional DC/DC converters used in EESS, there are three common topologies: basic buck/boost, interleaved buck/boost, and dual active bridge (DAB) [24]. The topology chosen in this paper is a six-phase interleaved DC/DC converter. With the interleaved DC/DC converter, it is possible to achieve no turn-on losses of the transistor, and the total inductor volume is smaller than the inductor volume in the basic buck/boost topology [39]. By reducing the volume of the DC/DC converter, the EESS can be more compact and fit into tighter spaces. The schematic of a six-phase interleaved DC/DC converter is shown in Figure 9. It consists of six phases, where each phase is constructed from a half-bridge and an inductor.

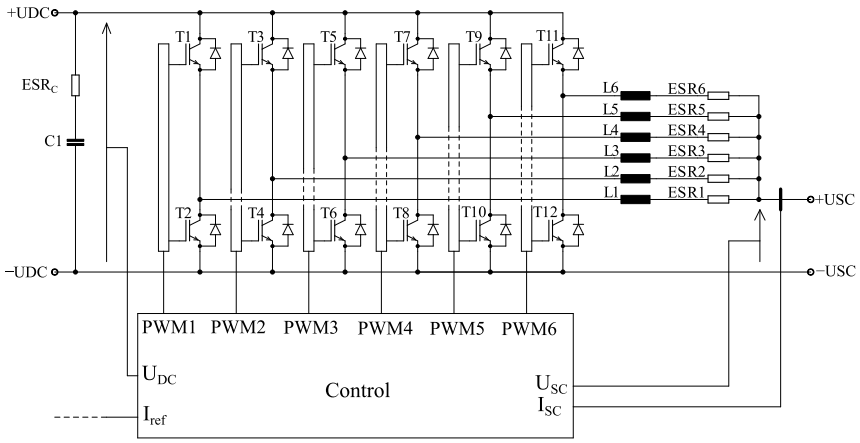

Figure 9. Schematic of a six-phase interleaved buck/boost DC/DC converter.

For the design of the DC/DC converter, the operating voltages and currents must be specified. The operating voltages of the DC/DC converter for the EESS under study are determined by the DC-link voltages of the elevator VFD (500–800 V) and the SC bank operating voltages (150–300 V). The current value is determined by the required peak power of the DC/DC converter. If the constant power of the supercapacitor is to be maintained over the full range of the operating voltage, the current must vary with the voltage. Therefore, the peak output power for the DC/DC converter used in the EESS was set at about 80 % of the nominal power of the elevator. In this case, this corresponds to a peak power of 8 kW. With a maximum supercapacitor voltage of 300 V, this results in an SC bank current of about 27 A.

The load of the DC/DC converter changes according to the requirements of the elevator, which are very dynamic. The dynamic load change of the DC/DC converter can affect the temperature change profile of the semiconductor. The dynamic load change of the DC/DC converter can affect the temperature change profile of the semiconductors. Continuous temperature changes of the semiconductors can shorten the lifetime of the semiconductors [40–42].

In the simulation model, the transistors are modeled as ideal, but the transistor conduction and switching losses are modeled with a variable current source connected to the DC

bus. In this way, the complexity of the simulation model is reduced, which helps increase the simulation speed. Considering all modeled losses, the efficiency of the DC/DC converter at maximum power and 600 V on the DC bus is approximately 95 %. The parameters of the modeled DC/DC converter are given in Table 3.

Table 3. DC/DC converter parameters.

Parameter	Value
Input voltage, U_{in} [V]	500–800
Output voltage, U_{out} [V]	150–300
Max. input current, I_{in} [A]	16
Output current, I_{out} [A]	0–27
Switching frequency, f_{sw} [kHz]	25
Inductance of inductor, L_1–L_6 [µH]	350
ESR, ESR1-ESR6 [Ω]	0.2

As described in [34], control of the interleaved DC/DC converter is achieved by a phase shift between the PWM signals controlling each phase with a phase shift of $2\pi/N$, where N is the number of phases. In this case, the phase shift is $\pi/3$. The PI controller is used to control the supercapacitor current by controlling the duty cycle of the PWM signal of each phase. Each mode (buck and boost) has its own PI controller to control the charge and discharge current of the SC bank. In buck mode, the T_{2n} transistors (for n in the range of 1 to 6) are turned off, while the T_{2n-1} transistors are controlled by PWM. In boost mode, it is the other way around: the T_{2n-1} transistors are turned off, while the T_{2n} transistors are controlled by PWM. In each mode, i.e., buck and boost, the SC bank current is measured, based on which the duty cycle for PWM is determined. To control each phase, each phase of the interleaved converter has its own PWM generator, which has a phase shift. Since the DC/DC converter must be able to switch between modes, the PI controller has a function to reset the integral function of the controller in each mode.

4.3. Control Circuit

The control circuit of the EESS is responsible for controlling the charging and discharging of the supercapacitor bank depending on the behaviour of the elevator. Several approaches to the use of control algorithms for EESS are described in the literature, including dynamic programming [15], fuzzy logic [17], rule-based (RB) [15] and PI controller [43]. In this paper, the control is achieved with a controller similar to the method proposed in [43], which uses the PI controller.

5. Simulation Results

The simulation model of the elevator system presented in Section 3 was extended to include the simulation model of the EESS presented in Section 4. The simulation model of the elevator system with EESS is shown in Figure 10. The simulation tests were performed under different operating conditions. The objective was to test the operation of the proposed energy storage solution and to estimate possible savings due to energy storage. The results of the following simulation tests are presented: operation during a reference cycle, operation during two consecutive regenerative trips, and operation under real traffic demand during a 7-min interval. In all the simulation tests, the stored energy was used for driving, but it could also be used for any other purpose. The results are evaluated as follows.

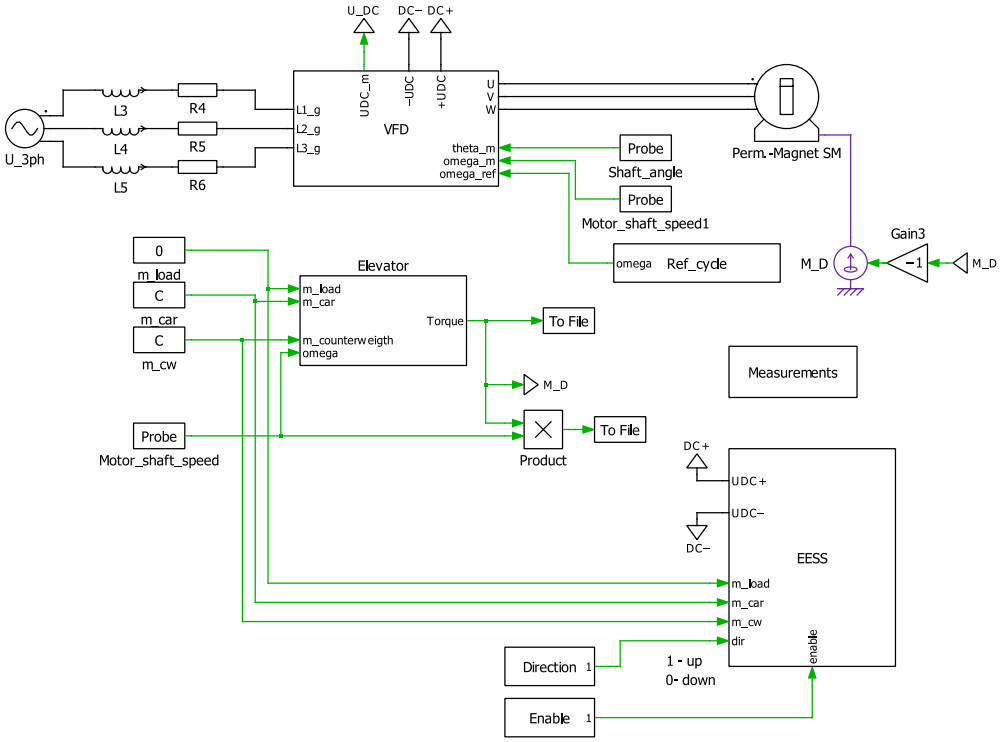

Figure 10. Simulation model of the elevator system with EESS.

5.1. Reference Cycle

The reference cycle consists of running an empty elevator from the ground floor to the top floor and vice versa. When the mass of the counterweight is equal to the sum of the mass of the car and 50% of the load, the reference cycle represents the elevator travel with the highest possible regenerative energy production (while the elevator travels from the ground floor to the top floor) and the highest possible energy consumption (while the elevator travels from the top floor to the ground floor). Therefore, high energy savings can be achieved during the reference cycle.

The speed setpoint and load profile during the reference cycle are shown in Figure 11a. The elevator first operates in regenerative mode and stores the energy in the SC bank, then it operates in motor mode and the energy is used for motor operation. The initial voltage of the supercapacitor bank was assumed to be 200 V. The reference voltage for the DC bus in EESS was set to 600 V. The results are shown in Figures 11 and 12. The energy consumption was compared with that of the elevator system without EESS.

The input power of the elevator system, with and without EESS, is shown in Figure 11b. It can be seen that the EESS reduces the peak power of the grid by about 43 %. Also, the total energy consumption of the elevator system with EESS is 103 kJ, while the total energy consumption without EESS is 215 kJ. With the EESS, an energy saving of about 52 % is achieved during the reference cycle.

The DC bus voltage is shown in Figure 12a. In regenerative mode, the DC bus voltage is about 650 V. At about 20 s, a regenerative power peak occurs, which shows up as a voltage peak of 720 V on the DC bus. This is due to the regenerative power being slightly higher than the value of the power that can be stored in the SC bank. In motor mode, the bus voltage drops from DC to about 530 V as the line voltage drops and the power consumed by the elevator is higher than the power supplied by the EESS.

The power of the SC bank and the power dissipation at the braking resistor are shown in Figure 12b. It can be observed that the power dissipation at the braking resistor occurs at about 20 s during the voltage peak on the DC bus (Figure 12a). When the SC bank accumulates energy, the SC bank power is positive. When the SC bank dissipates energy, the power of the SC bank is negative. In regenerative mode, the power of the SC bank is

constant until the maximum regenerative power is reached. In motor mode, the power of the SC bank decreases over time.

The current and voltage of the SC bank are shown in Figure 12c; when the SC bank accumulates energy, the current is positive, and when it dissipates energy, it is negative. In a regenerative mode, the SC bank current decreases while the SC bank voltage increases. The result is the constant power of the SC bank. In an elevator motor mode, the current of the SC bank is constant, while the voltage decreases.

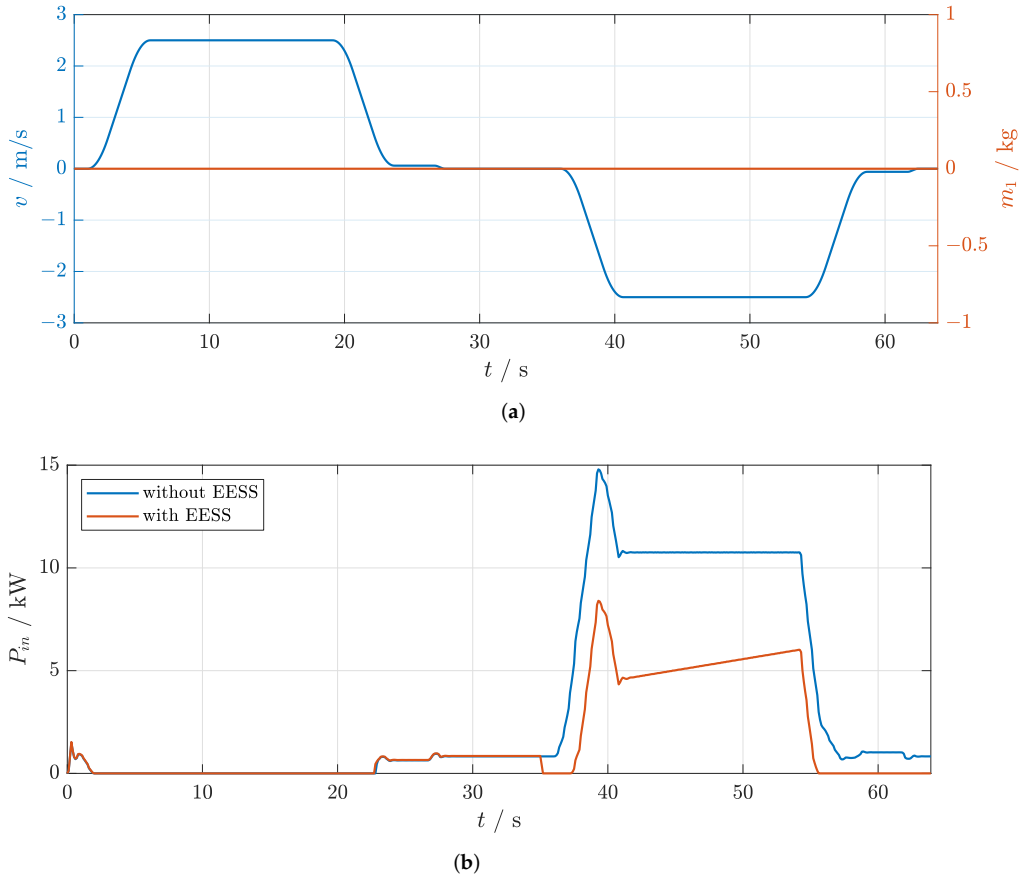

Figure 11. Simulation results for the reference cycle. (**a**) Elevator speed setpoint and mass of the load. (**b**) Input power.

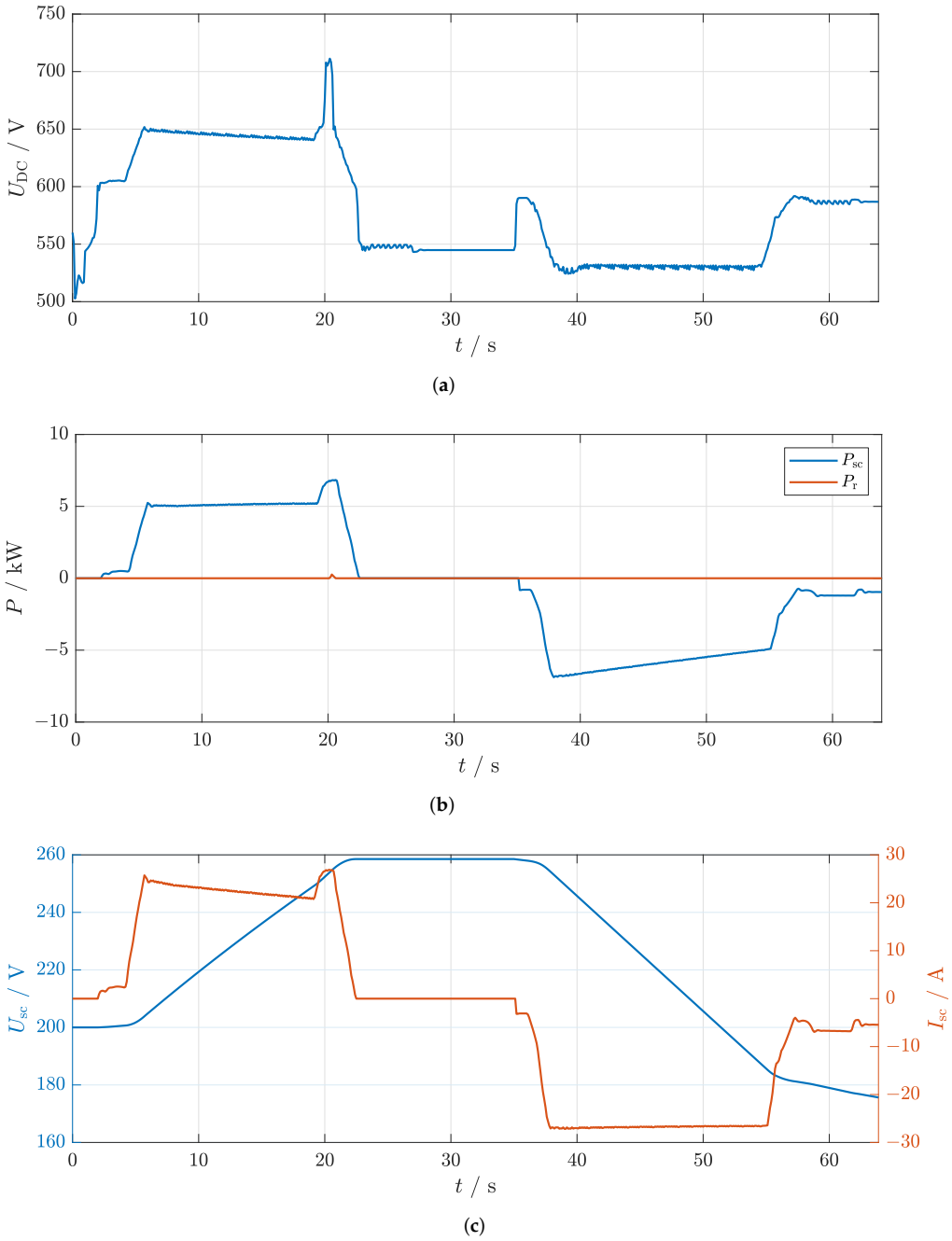

Figure 12. Simulation results for the reference cycle. (**a**) DC bus voltage. (**b**) SC bank power and braking resistor power. (**c**) Voltage and current of the SC bank.

5.2. Consecutive Regenerative Trips

Simulation tests were performed for two consecutive regenerative trips with maximum regenerative energy, since the SC bank is dimensioned to save the energy for this case. The initial voltage of the SC bank was assumed to be 155 V, which is slightly higher than the lower limit of the operating voltage of the SC bank. The simulation was performed as a reference cycle where the empty elevator travels from the ground floor to the top floor and from the top floor to the ground floor with the nominal load. Figure 13a shows the speed setpoint and load profile during two consecutive regenerative trips. A positive speed indicates an upward movement of the elevator car, while a negative sign represents a downward movement.

The input power of the elevator system with and without EESS is shown in Figure 13b. During two consecutive regenerative trips, the elevator operates in regenerative mode and the power from the grid is almost the same for the elevator system with and without EESS. However, since the EESS has a standby power of 24 W, the consumed power with EESS is slightly higher than the power without EESS. In addition, a power disturbance is observed at 35 s because the elevator load has changed and the mechanical brake is not simulated.

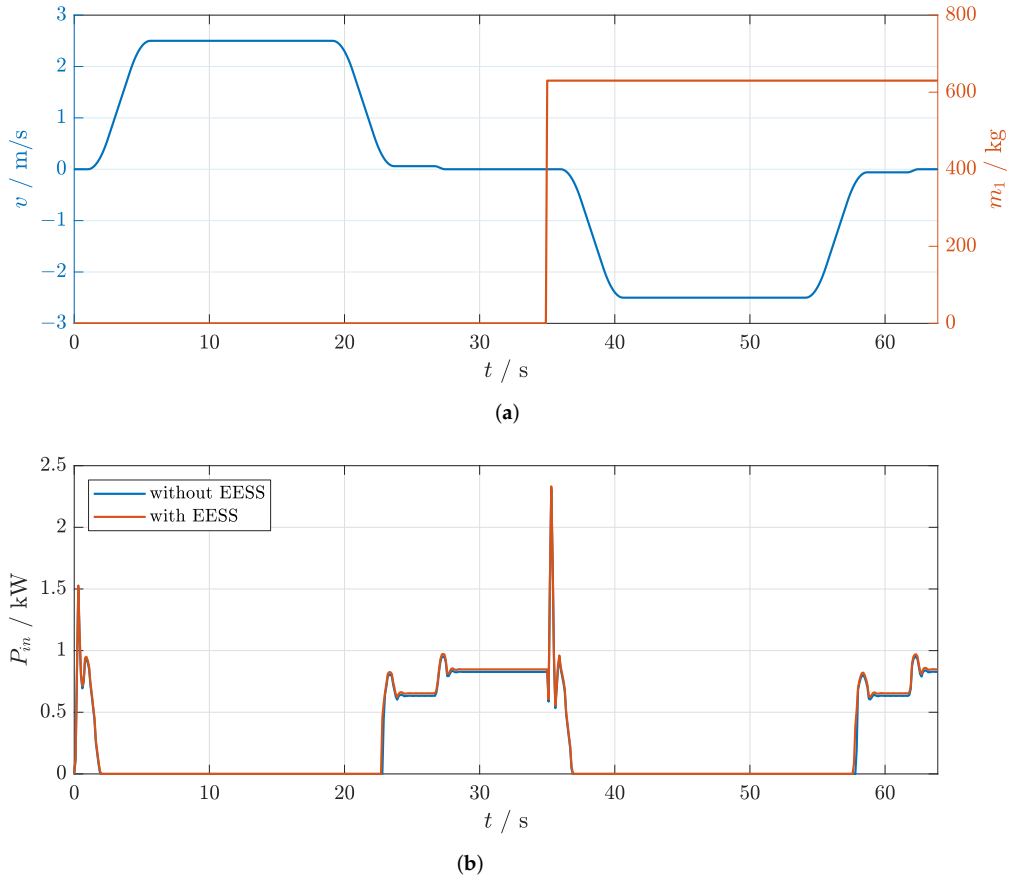

Figure 13. Simulation results for two consecutive regenerative trips. (**a**) Elevator speed setpoint and mass of the load. (**b**) Input power.

The DC bus voltage is shown in Figure 14a. During the first regenerative trip, the DC bus voltage increases to 720 V, which means that the SC bank is not able to store all the regenerative energy, and there is a power dissipation at the braking resistor. Since the braking resistor is controlled by a relay with hysteresis, there is a voltage fluctuation on the DC bus. During the second regenerative trip, the DC bus voltage is about 650 V, and all the regenerative energy is stored in the SC bank.

The power of the SC bank and the power of the braking resistor are shown in Figure 14b. During the first regenerative trip, there is power dissipation at the braking resistor. During the second trip, there is no power dissipation at the braking resistor, and the power of the SC bank is constant and equal to the regenerative power of the elevator.

The current and voltage of the SC bank are shown in Figure 14c. During the first regenerative trip, the current of the SC bank reaches its maximum value of 27 A. This means that the charging power of the SC bank is limited by the maximum charging current of the DC/DC converter.

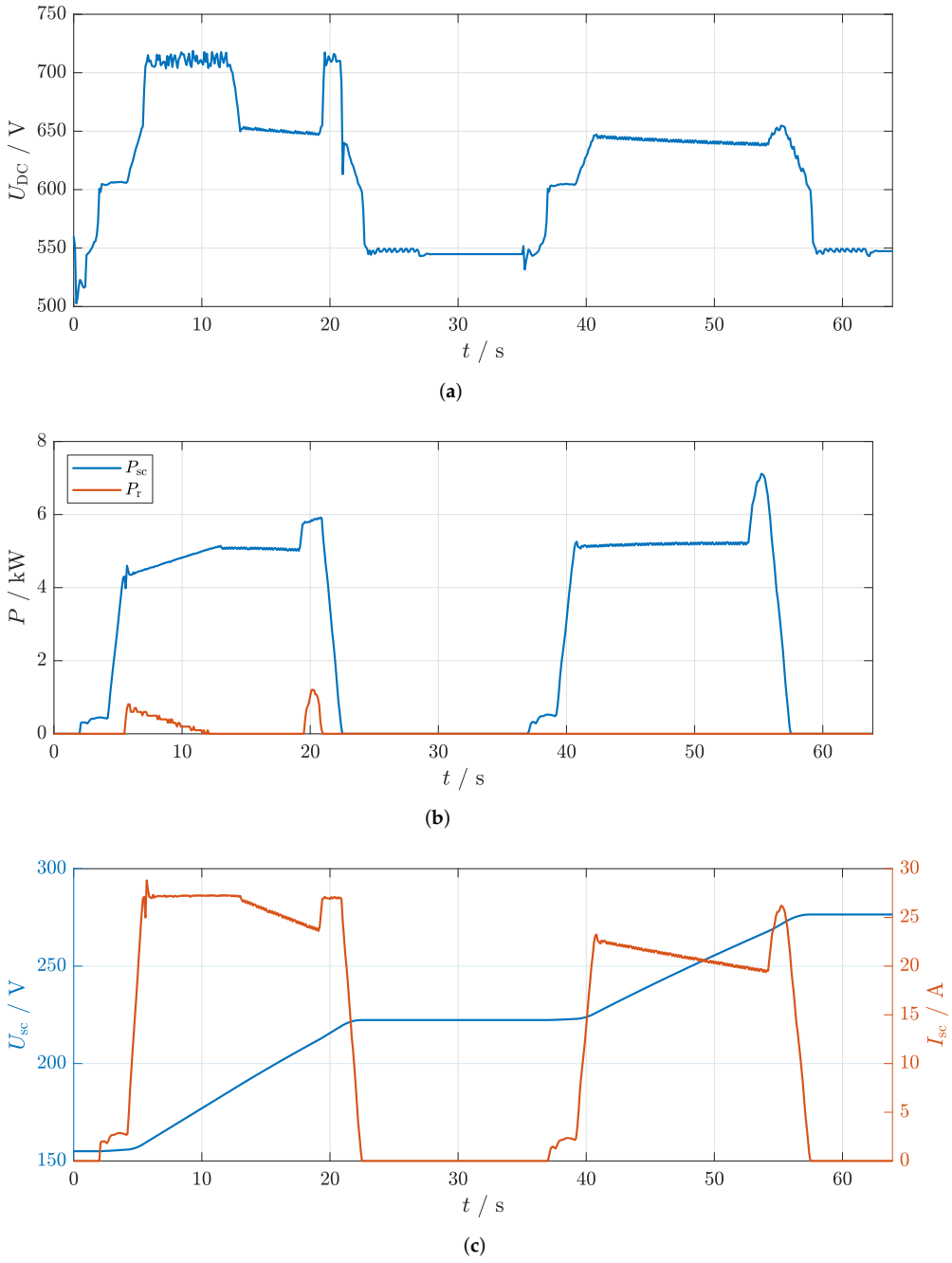

Figure 14. Simulation results for two consecutive regenerative trips. (**a**) DC bus voltage. (**b**) SC bank power and braking resistor power. (**c**) Voltage and current of the SC bank.

5.3. Real Traffic Data

The simulation test was performed with real traffic data obtained during the field measurement at the faculty elevator. The speed setpoint, load, and power consumption were measured for one day. The measured speed setpoint and load profile were the inputs to the simulation model. The simulation results for randomly selected 7 min of traffic data are shown in Figures 15 and 16. The speed setpoint and load profile during the selected 7-min interval are shown in Figure 15a. It can be seen that there were twelve elevator trips with different loads during the selected interval. The initial voltage of the SC was set to 200 V.

The total energy consumption during the selected 7-min interval of the elevator system without EESS was 895 kJ, while the energy consumption of the elevator system with EESS

was 581 kJ. Thus, an energy saving of 35% was achieved with the EESS. In addition, the peak power of the elevator system without EESS was 14.7 kW, while the peak power of the elevator system with EESS was 11.5 kW, resulting in a peak power reduction of 22%.

The input power of the elevator system with and without EESS is shown in Figure 15b. The use of EESS reduced the power consumption from the grid. From 600 s to 630 s, the SC bank was discharged, so it could not reduce the power consumption from the grid for this particular elevator trip.

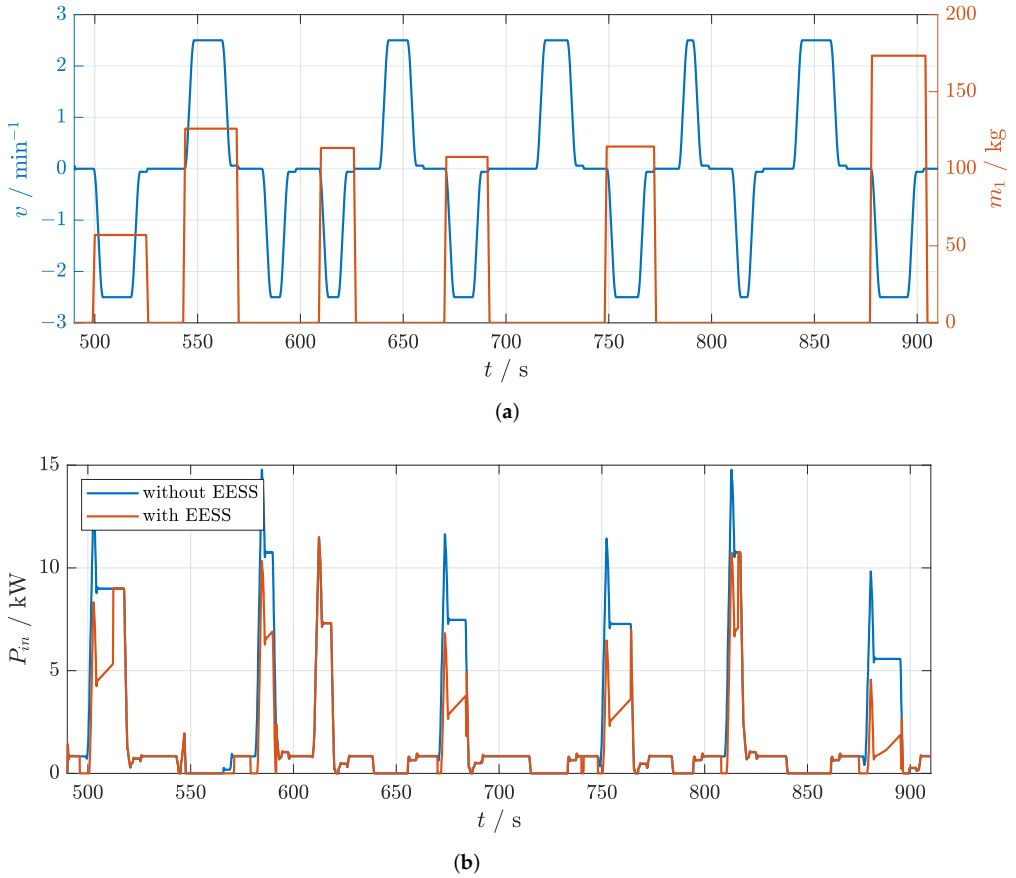

Figure 15. Simulation results for real traffic data. (**a**) Elevator speed setpoint and mass of the load. (**b**) Input power.

The DC bus voltage is shown in Figure 16a. It can be observed that, in some cases, the voltage on the DC bus increased to 720 V, which means that the SC bank could not store all the available regenerative energy and there was a power dissipation at the braking resistor.

The power of the SC bank and the power of the braking resistor are shown in Figure 16b. It can be seen that the SC bank was not able to store the current regenerative energy at some moments, resulting in power dissipation at the braking resistor. The SC bank was not able to store all the energy due to the low voltage of the SC bank and the current limiting the maximum power value at lower voltages.

The voltage and current of the SC bank are shown in Figure 16. It can be seen that the SC bank was emptied to the lower limit and its current was, at times, at the limit.

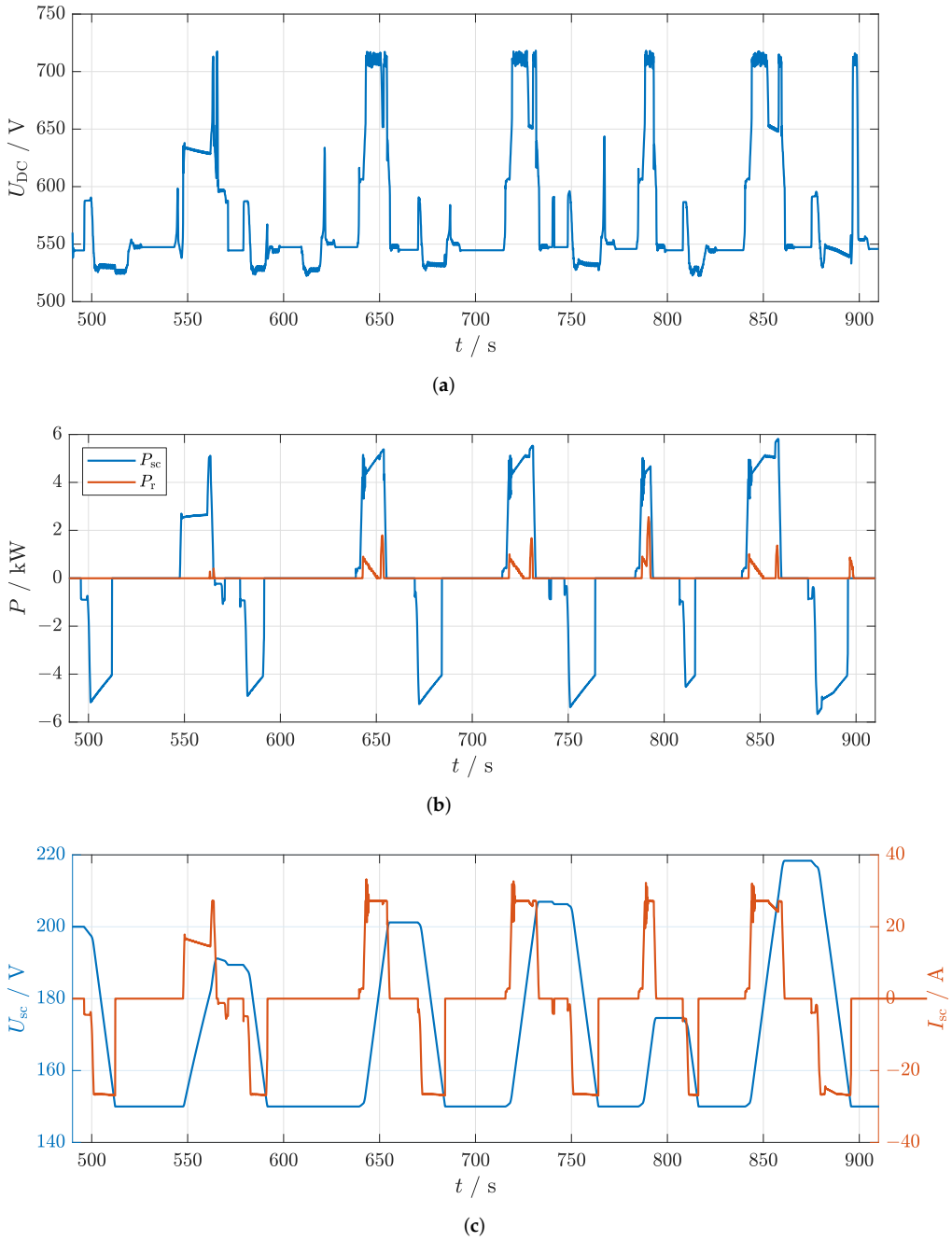

Figure 16. Simulation results for real traffic data. (**a**) DC bus voltage. (**b**) SC bank power and braking resistor power. (**c**) Voltage and current of the SC bank.

6. Discussion

The simulation results showed that significant energy savings can be achieved with EESS. During the reference cycle, which is the elevator trip with high possible energy savings, energy savings of up to 52% were achieved, with a 43% reduction in the peak power of the grid. When real traffic data from on-site measurements were used as input to the simulation model, the simulation results showed energy savings of 35% and a reduction in the peak power of the grid by 22%. The energy savings are highly dependent on elevator traffic, which is inherently stochastic. The energy stored in the SC bank depends on the frequency of elevator trips, the type of trips (regenerative or motor), the duration, and the arrangement of regenerative and motor trips. The energy savings achieved also depend on the control algorithms. Higher energy savings can be achieved if the dispatch algorithm

maximises stored energy. Higher peak power reduction can also be achieved by a different control approach, where the EESS provides energy mainly during the acceleration time of the elevator.

The simulation results during the two consecutive regenerative trips have shown that it is impossible to achieve the same nominal power for each SC bank voltage due to the voltage fluctuations of the SC bank and the maximum output current of the DC/DC converter. For this reason, even though the SC bank was not fully charged and was designed for two regenerative trips with maximum energy, power dissipation occurred at the braking resistor during two consecutive regenerative trips. By increasing the output current capacity of the DC/DC converter , it would be possible to store all the regenerative energy in the SC bank, which could increase the overall efficiency of the elevator system, but also increase the cost.

Simulation results also confirmed the effectiveness of the proposed EESS. Most of the regenerative energy was stored in the SC bank and effectively used during the motor mode. Due to the current limitation of the DC/DC converter, power dissipation at the braking resistor occurred when the voltage of the SC bank was lower or the SC bank was fully charged.

The elevator system with the EESS can achieve significant energy savings in a building and provide additional functionality because the energy storage can be used to supply other equipment. Integrating the elevator system with the EESS into the building management system (BMS) could provide a quick and controllable energy source and storage, further improving the energy efficiency of the building. Renewable energy sources, such as solar panels, can also be connected to the energy storage system, creating an elevator with a positive energy balance.

Future work will focus on exploring potential energy savings in a group of elevators where higher energy savings may be possible and on exploring control algorithms that could further improve energy savings. In addition, the prototype of the proposed EESS will be validated through experimental testing.

7. Conclusions

An efficient elevator system can significantly improve the energy efficiency of a building. One way to improve the efficiency of the elevator system is to use regenerative energy. In this paper, a supercapacitor-based energy storage system for elevator applications was proposed, and a comprehensive study of the energy savings achieved by the proposed system was conducted. The energy storage system consists of a supercapacitor bank and a bidirectional six-phase interleaved DC/DC converter. The energy storage system was modeled considering all physical constraints. In addition, simulation tests were performed using the simulation model of the existing elevator system, which was verified with on-site measurements. The verified simulation model ensures that the simulation results are very close to the measurement results, and a reliable energy savings study can be performed. The simulation tests were conducted under different operating conditions, and the results of the reference cycle, two consecutive regenerative trips, and real traffic data are presented and analysed. The simulation results showed the effectiveness of the proposed energy storage system, and the energy saving study showed that the proposed system can achieve significant energy savings. Moreover, the proposed system can add new functionalities to energy-efficient buildings.

Author Contributions: Conceptualization, M.M. and M.K.; methodology, M.M. and L.P.; validation, M.M. and L.P.; investigation, M.M.; resources, L.P.; writing—original draft preparation, M.M. and M.K.; writing—review and editing, M.M., M.K. and L.P.; visualization, M.M. and L.P.; supervision, M.K. All authors have read and agreed to the published version of the manuscript.

Funding: This work has been fully supported by the European Regional Development Fund under the project EULIFT-Development of a Smart Modular Elevator Drive System for Increasing the Energy Efficiency of a Building (EFRR-IRI-II-KK.01.2.1.02.0077).

Institutional Review Board Statement: Not applicable.

Informed Consent Statement: Not applicable.

Data Availability Statement: The data presented in this study are available on request from the corresponding author.

Conflicts of Interest: The authors declare no conflict of interest.

Abbreviations

The following abbreviations are used in this manuscript:

ZEB	Zero Energy Building
PEB	Positive Energy Building
MRL	Machine-roomless
VFD	Variable Frequency Drive
EESS	Elevator Energy Storage System
SC	Supercapacitor
FOC	Field-Oriented Control
ESR	Equivalent Series Resistance

Appendix A

Table A1. Elevator data.

Parameter	Value
Nominal load, Q [kg]	630
Nominal speed, v_N [m/s]	2.5
Car weight [kg]	800
Counterweight compensation [%]	50
Operating days per year, d_{op}	365
Lifting height, F_H [m]	45.6
Number of floors	13
Maximum number of passengers	8

Table A2. VFD data.

Parameter	Value
Load factor at I_n, L_f [%]	60
Nominal power, P_n [kW]	12.1/8.4
Nominal voltage, U_n [V]	400
Nominal current, I_n [A]	32
Peak current, I_p [A]	52
Switching frequency, P_{sw} [kHz]	4–16
Weight, m_{VFD} [kg]	16.4

Table A3. Motor data.

Parameter	Value
Duty cycle, D [%]	S3-20/40
Nominal power, P_n [kW]	12.1/8.4
Nominal voltage, U_n [V]	360
Nominal current, I_n [A]	32/22
Nominal speed, n_n [min^{-1}]	192
Power factor, $cos\phi$	0.9/0.95
Inertia, J_m [$kg{\cdot}m^2$]	0.31
Stator resistance, R_s [Ω]	0.67
Induced voltage, U_g [V]	222
Nominal torque, T_n [Nm]	600/420

References

1. Shukla, A.; Sharma, A. *Sustainability Through Energy-Efficient Buildings*; CRC Press: Boca Raton, FL, USA, 2018.
2. D'Agostino, D.; Mazzarella, L. What is a Nearly zero energy building? Overview, implementation and comparison of definitions. *J. Build. Eng.* **2019**, *21*, 200–212. [CrossRef]
3. Magrini, A.; Lentini, G.; Cuman, S.; Bodrato, A.; Marenco, L. From nearly zero energy buildings (NZEB) to positive energy buildings (PEB): The next challenge-The most recent European trends with some notes on the energy analysis of a forerunner PEB example. *Dev. Built Environ.* **2020**, *3*, 100019. [CrossRef]
4. Deng, S.; Wang, R.Z.; Dai, Y.J. How to evaluate performance of net zero energy building—A literature research. *Energy* **2014**, *71*, 1–16. [CrossRef]
5. Wilberforce, T.; Olabi, A.G.; Sayed, E.T.; Elsaid, K.; Maghrabie, H.M.; Abdelkareem, M.A. A review on zero energy buildings–Pros and cons. *Energy Built Environ.* **2021**. [CrossRef]
6. Ang, J.H.; Yusup, Y.; Zaki, S.A.; Salehabadi, A.; Ahmad, M.I. Comprehensive Energy Consumption of Elevator Systems Based on Hybrid Approach of Measurement and Calculation in Low-and High-Rise Buildings of Tropical Climate towards Energy Efficiency. *Sustainability* **2022**, *14*, 4779. [CrossRef]
7. Al-Kodmany, K. Tall buildings and elevators: A review of recent technological advances. *Buildings* **2015**, *5*, 1070–1104. [CrossRef]
8. Liu, H.P.; Liu, K.; Sun, B.N. Analysis of energy management strategy for energy-storage type elevator based on supercapacitor. In Proceedings of the 2017 11th IEEE International Conference on Compatibility, Power Electronics and Power Engineering (CPE-POWERENG), Cadiz, Spain, 4–6 April 2017; pp. 175–180.
9. Nemeth, B.; Place, H. *Energy-Efficient Elevator Machines*; ThyssenKrupp Elevator: Frisco, TX, USA, 2011.
10. Nipkow, J.; Schalcher, M. Energy consumption and efficiency potentials of lifts. *Hospitals* **2006**, *2*, 3.
11. Sachs, H.; Misuriello, H.; Kwatra, S. *Advancing Elevator Energy Efficiency*; Report A1501; American Council for an Energy-Efficient Economy: Washington, DC, USA, 2015.
12. Kafalis, K.; Karlis, A.D. Comparison of flywheels and supercapacitors for energy saving in elevators. In Proceedings of the 2016 IEEE Industry Applications Society Annual Meeting, Portland, OR, USA, 2–6 October 2016; pp. 1–8.
13. Mathew, S.; Mogre, P.; Chouthai, R.; Karandikar, P.; Kulkarni, N. Supercapacitor based energy recovery system for an elevator. In Proceedings of the 2017 International Conference on Advances in Computing, Communication and Control (ICAC3), Mumbai, India, 1–2 December 2017; pp. 1–5.
14. Luri, S.; Etxeberria-Otadui, I.; Rujas, A.; Bilbao, E.; González, A. Design of a supercapacitor based storage system for improved elevator applications. In Proceedings of the 2010 IEEE Energy Conversion Congress and Exposition (ECCE) , Atlanta, GA, USA, 12–16 September 2010; Communication and Control (ICAC3), pp. 4534–4539.
15. Bilbao, E.; Barrade, P.; Etxeberria-Otadui, I.; Rufer, A.; Luri, S.; Gil, I. Optimal energy management of an improved elevator with energy storage capacity based on dynamic programming. In Proceedings of the 2012 IEEE Energy Conversion Congress and Exposition (ECCE), Raleigh, NC, USA, 15–20 September 2012; pp. 3479–3484.
16. Attaianese, C.; Nardi, V.; Parillo, F.; Tomasso, G. High performances supercapacitor recovery system including Power Factor Correction (PFC) for elevators. In Proceedings of the 2007 European Conference on Power Electronics and Applications, Aalborg, Denmark, 2–5 September 2007; pp. 1–10.
17. Jabbour, N.; Mademlis, C. Improved control strategy of a supercapacitor-based energy recovery system for elevator applications. *IEEE Trans. Power Electron.* **2016**, *31*, 8398–8408. [CrossRef]
18. Kafalis, K.; Karlis, A. Supercapacitors based energy saving mode of electromechanical elevator's operation. In Proceedings of the 2016 XXII International Conference on Electrical Machines (ICEM), Lausanne, Switzerland, 4–7 September 2016; pp. 1208–1214.
19. Jabbour, N.; Mademlis, C. Supercapacitor-based energy recovery system with improved power control and energy management for elevator applications. *IEEE Trans. Power Electron.* **2017**, *32*, 9389–9399. [CrossRef]
20. Kubade, P.; Umathe, S. Enhancing an elevator efficiency by using supercapacitor. In Proceedings of the 2017 Third International Conference on Advances in Electrical, Electronics, Information, Communication and Bio-Informatics (AEEICB), Chennai, India, 27–28 February 2017; pp. 502–505.

21. Oyarbide, E.; Elizondo, I.; Martínez-Iturbe, A.; Bernal, C.; Irisarri, J. Ultracapacitor-based plug & play energy-recovery system for elevator retrofit. In Proceedings of the 2011 IEEE International Symposium on Industrial Electronics (ISIE) , Gdansk, Poland, 27–30 June 2011; pp. 462–467.
22. Nobile, G.; Sciacca, A.G.; Cacciato, M.; Cavallaro, C.; Raciti, A.; Scarcella, G.; Scelba, G. Energy harvesting in roped elevators. In Proceedings of the 2014 International Symposium on Power Electronics, Electrical Drives, Automation and Motion (SPEEDAM) , Ischia, Italy, 18–20 June 2014; pp. 533–540.
23. Rufer, A.; Barrade, P. A supercapacitor-based energy-storage system for elevators with soft commutated interface. *IEEE Trans. Ind. Appl.* **2002**, *38*, 1151–1159. [CrossRef]
24. Makar, M.; Kutija, M.; Pravica, L.; Jukić, F. DC/DC Converter Topologies for Elevator Energy Storage Systems Based on Supercapacitors. In Proceedings of the 2021 International Conference on Electrical Drives & Power Electronics (EDPE), Dubrovnik, Croatia, 22–24 September 2021; pp. 220–227.
25. Kermani, M.; Shirdare, E.; Abbasi, S.; Parise, G.; Martirano, L. Elevator Regenerative Energy Applications with Ultracapacitor and Battery Energy Storage Systems in Complex Buildings. *Energies* **2021**, *14*, 3259. [CrossRef]
26. Zhang, Y.; Yan, Z.; Yuan, F.; Yao, J.; Ding, B. A novel reconstruction approach to elevator energy conservation based on a DC micro-grid in high-rise buildings. *Energies* **2018**, *12*, 33. [CrossRef]
27. Abad, G. *Power Electronics and Electric Drives for Traction Applications*; John Wiley & Sons: Hoboken, NJ, USA, 2016.
28. Kulkarni, A.B.; Nguyen, H.; Gaudet, E. A comparative evaluation of fine regenerative and nonregenerative vector controlled drives for AC gearless elevators. In Proceedings of the 2000 IEEE Industry Applications Conference. Thirty-Fifth IAS Annual Meeting and World Conference on Industrial Applications of Electrical Energy (Cat. No. 00CH37129), Rome, Italy, 8–12 October 2000; Volume 3, pp. 1431–1437.
29. Kutija, M.; Pravica, L.; Godec, D.; Erica, D. Regenerative energy potential of roped elevator systems-a case study. In Proceedings of the 2021 IEEE 19th International Power Electronics and Motion Control Conference (PEMC), Gliwice, Poland, 25–29 April 2021; pp. 284–291.
30. Wang, L.; Chai, S.; Yoo, D.; Gan, L.; Ng, K. *PID And Predictive Control of Electrical Drives and Power Converters Using MATLAB/Simulink*; John Wiley & Sons: Hoboken, NJ, USA, 2015.
31. Erica, D.; Godec, D.; Kutija, M.; Pravica, L.; Pavlić, I. Analysis of Regenerative Cycles and Energy Efficiency of Regenerative Elevators. In Proceedings of the 2021 International Conference on Electrical Drives & Power Electronics (EDPE), Dubrovnik, Croatia, 22–24 September 2021; pp. 212–219.
32. Soylu, S. *Electric Vehicles: Modelling and Simulations*; IntechOpen: London, UK, 2011.
33. Yu, A.; Chabot, V.; Zhang, J. *Electrochemical Supercapacitors for Energy Storage and Delivery: Fundamentals and Applications*; Taylor & Francis: Abingdon, UK, 2013.
34. Grbovic, P.J. *Ultra-Capacitors in Power Conversion Systems: Applications, Analysis, and Design From Theory to Practice*; John Wiley & Sons: Hoboken, NJ, USA, 2013.
35. Doljack, F.A.; Schultz, N.; Kamath, H.P.; Strain, J. Active Balancing Modular Circuits. U.S. Patent 7,342,768 B2, 11 March 2008.
36. Du, L. Study on supercapacitor equivalent circuit model for power electronics applications. In Proceedings of the 2009 2nd International Conference on Power Electronics and Intelligent Transportation System (PEITS), Shenzhen, China, 19–20 December 2009; Volume 2, pp. 51–54.
37. Kularatna, N. *Energy Storage Devices for Electronic Systems: Rechargeable Batteries and Supercapacitors Energy Storage Devices for Electronic Systems: Rechargeable Batteries and Supercapacitors*; School of Engineering, The University of Waikato 581 Hamilton: Hamilton, New Zealand, 2014.
38. Xiong, G.; Kundu, A.; Fisher, T.S. *Thermal Effects in Supercapacitors*; Springer: Berlin, Germany, 2015.
39. Destraz, B.; Louvrier, Y.; Rufer, A. High efficient interleaved multi-channel dc/dc converter dedicated to mobile applications. In Proceedings of the 2006 IEEE Industry Applications Conference Forty-First IAS Annual Meeting, Tampa, FL, USA, 8–12 October 2006; Volume 5, pp. 2518–2523.
40. Sarkany, Z.; He, W.; Rencz, M. Temperature change induced degradation of SiC MOSFET devices. In Proceedings of the 2016 15th IEEE Intersociety Conference on Thermal and Thermomechanical Phenomena in Electronic Systems (ITherm), Las Vegas, NV, USA, 31 May–3 June 2016; pp. 1572–1579.
41. Herrmann, T.; Feller, M.; Lutz, J.; Bayerer, R.; Licht, T. Power cycling induced failure mechanisms in solder layers. In Proceedings of the 2007 European Conference on Power Electronics and Applications, Aalborg, Denmark, 2–5 September 2007; pp. 1–7.
42. Bayerer, R.; Herrmann, T.; Licht, T.; Lutz, J.; Feller, M. Model for power cycling lifetime of IGBT modules-various factors influencing lifetime. In Proceedings of the 5th International Conference on Integrated Power Electronics Systems, VDE, Nuremberg, Germany, 11–13 March 2008; pp. 1–6.
43. Lin, S.; Song, W.; Chen, Y.; Luo, L.; Feng, Z. Study on the model of elevator regeneration energy and its energy storage control method. In Proceedings of the 2015 International Conference on Smart Grid and Clean Energy Technologies (ICSGCE), Offenburg, Germany, 20–23 October 2015; pp. 125–128.